Solitary waves and controllable dynamical chaos in the case of parametric interaction

G. N. Burlak and K. Ishkabulov

Taras Shevchenko Kiev University, 252127 Kiev, Ukraine
(Submitted 25 August 1995)
Zh. Éksp. Teor. Fiz. **109**, 774–785 (March 1996)

A study is made of acoustooptical interaction in a strongly nonlinear regime. It is shown that the presence of multiple wave reflection, which plays the role of delayed feedback, gives rise in the system to soliton dynamics that lead to the formation of spatially inhomogeneous structures and to periodic fluctuations of the amplitudes at the output. An increase in supercriticality leads to the generation of an appreciable nonsoliton part and, accordingly, to the formation of regions of wide-band irregular oscillations. It is found that modulation of the pump wave amplitude plays an active role in the formation of chaotic regimes. © *1996 American Institute of Physics.* [S1063-7761(96)00503-6]

1. INTRODUCTION

In recent years, effects associated with the phenomenon of self-organization have attracted much attention in the study of nonlinear wave systems.[1–4] The main interest attaches to systems in which both coherent and chaotic regimes can arise from variation of external parameters as a result of space–time evolution. A typical situation occurs in the investigation of the transition of a nonlinear medium that is above the instability threshold to different spatially inhomogeneous states. In the general case, the controlling parameter changes in time (or in space) as a result of external factors. If as a result the range of its values passes through the critical zone, the external influences begin to play an active role, since the dynamics of the system at different instants of time may become either regular or chaotic.

The study in Refs. 3 and 4 of a single-mode laser with delayed feedback revealed the presence of complicated dynamics that lead to the formation of spatial structures of phase defects. An output signal taking the form of regular oscillations with constant amplitude and constant phase was studied in the case of subcritical conditions. However, in the above-threshold regime losses of phase coherence in the oscillations are observed, their number increasing rapidly with increasing supercriticality.

In the analysis of this phenomenon, the time series of the output channel (one-dimensional) is transformed by means of the well-known procedure to a quasi-space–time representation (two-dimensional). Analysis of this representation led to conclusions about the details of the space–time dynamics in the system.

At the same time, in interpreting the observed dependences, the authors of Ref. 3, using the criticality of the phenomenon, invoked the spatially homogeneous version of the Ginzburg–Landau model augmented with a term corresponding to delayed feedback. However, it is clear that such an approach does not always give sufficient accuracy.

First, it can at best give only qualitative agreement, since in such a case the parameters of the model are not readily related to the physical parameters of an experiment. Second, the actual space–time dynamics of the nonlinear process, the details of which determine its fundamental properties as a whole, here escape consideration. Third, it is necessary to investigate the possibility of such a phenomenon in the framework of a model of the resonant interaction of light with matter, which is closer to the physics of the phenomenon.[5]

We note that at the present time the properties of bounded systems with allowance for soliton dynamics, wave absorption, and delayed feedback have not been sufficiently studied.[1,2] Moreover, it is important to investigate not only a model problem but also a very simple system that possesses the indicated properties and admits experimental realization.

In this paper, we have investigated nonlinear acoustooptical interaction in a crystal in the soliton regime with allowance for reflection from the boundaries, which plays the role of delayed feedback. We show that a steady state is established in the system at low supercriticalities. However, above a certain threshold a new dynamical state arises that does not evolve to any steady-state distribution. When the threshold is slightly exceeded, the generated solitons form a dynamical structure that gives rise to periodic oscillations at the output. Farther above the threshold, the soliton trajectories are distorted, and the periodic regime becomes more complicated. A further increase of the supercriticality leads to the occurrence of dynamical chaos. However, if the parameters of the system, for example the modulation of the pump wave, vary in time, then in the interaction process transitions between these regimes are possible.

2. BASIC EQUATIONS

We consider parallel acoustooptical interaction in an optically anisotropic crystal of the type of $LiNbO_3$. Suppose that along the z axis ordinary and extraordinary electromagnetic waves propagate and interact with a longitudinal acoustic wave at the difference frequency $\Omega=\omega_1-\omega_2$, $K=k_1-k_2$. It was shown in Ref. 6 that a soliton regime can arise in the presence of such an interaction in a partially unbounded crystal. In Ref. 7, localization of a coupled optical component of acoustooptical solitons was observed.

The equations of motion consist of Maxwell's equations and the equations of elasticity theory.

We consider a bounded crystal of length L with coeffi-

 1063-7761/96/030416-08$10.00

cients of reflection of sound $R_{0,L}$ at $z=0$, L, respectively. For simplicity, we shall in what follows neglect the reflection and absorption of the electromagnetic waves, which is weak in the transparency region. The system of equations obtained by the usual method for slowly varying wave amplitudes is augmented by the equation for the backward (reflected) acoustic wave, which by virtue of the conditions of mode locking does not interact with the field. The dynamics of the process is studied on the acoustic time scale, and therefore we ignore the time derivatives in the equations for the electromagnetic amplitudes in accordance with the parameter $s/c \approx 10^{-5} \ll 1$, where s and c are the speed of sound and light in the crystal. In what follows, we shall use the dimensionless form of the equations. As space and time scales, we choose $l_n = \sqrt{\alpha/E_0 K k_2}$ and l_n/s, respectively, where E_0 is the amplitude of the pump wave at the input, and α depends only on the parameters of the material. We also use a dimensionless coordinate and dimensionless time: $\zeta = z/l_n$ and $\tau = ts/l_n$, $l = L/l_n$.

The equations of motion for the dimensionless amplitudes (A_1 and A_2 are the amplitudes of the pump and idler electromagnetic waves, respectively, and A_3 and A_3' are the amplitudes of the direct and reflected acoustic waves, respectively) have the form

$$\frac{\partial}{\partial \zeta} A_{1,2} = \mp A_{2,1} A_3, \quad \left(\frac{\partial}{\partial \zeta} + \frac{\partial}{\partial \tau} + \gamma \right) A_3 = A_1 A_2,$$
$$\left(-\frac{\partial}{\partial \zeta} + \frac{\partial}{\partial \tau} + \gamma \right) A_3' = 0 \qquad (1)$$

with boundary and initial conditions

$$A_3(0,\tau) = f_3(\tau) + R_0 A_3'(0,\tau), \quad A_3'(l,\tau) = R_l A_3(l,\tau),$$
$$A_3(\zeta,0) = A_{30}(\zeta), \quad A_{1,2}(0,\tau) = f_{1,2}(\tau),$$

where $f_{1,2,3}(\tau)$ are the input signals. From the final equation in (1), we can find the amplitude of the reverse acoustic wave in the form

$$A_3'(\zeta,\tau) = R_l \exp[-\gamma(1-\zeta)] A_3(l, \zeta + \tau - l),$$

where $\gamma = \Gamma l_n$, in which Γ is the coefficient of absorption of sound.

With allowance for the relations $A_1^2 + A_2^2 = g^2(\tau) = f_1^2(\tau) + f_2^2(\tau)$, $A_1 = g(\tau)\cos\varphi$, $A_2 = g(\tau)\sin\varphi$, $A_3 = \partial\varphi/\partial\zeta$, the order of the system (1) can be reduced. After elimination of the amplitude A_3' of the reverse wave, the closed system of equations for φ and A_3, and also the boundary and initial conditions for them take the form

$$\left(\frac{\partial}{\partial \zeta} + \frac{\partial}{\partial \tau} + \gamma \right) A_3 = 0.5 g^2(\tau) \sin(2\varphi),$$
$$\varphi = \int_0^{\zeta} A_3(\zeta,\tau) d\zeta + \tan^{-1}\left(\frac{f_2(\tau)}{f_1(\tau)} \right), \qquad (2)$$

where $A_3(0,\tau) = f_3(\tau) + R^2 \exp(-\gamma l) A_3(l, \tau - l)$, $A_3(\zeta,0) = A_{30}(\zeta)$, $R^2 = R_0 R_l \leq 1$. It is important that the boundary modulation of the electromagnetic waves has directly entered Eq. (2) as a variable coefficient of the nonlinearity. This opens up the possibility of controlling the regimes of the nonlinear system.

Note that by the substitution

$$\left. \begin{matrix} u \\ v \end{matrix} \right\} = b(\zeta - \tau) \pm \frac{1}{b} \int g^2(\tau) d\tau, \quad \psi = 2\varphi, \quad b = \text{const}$$

we can reduce the system (2) to an equation of sine–Gordon type:

$$\frac{\partial^2 \psi}{\partial u^2} - \frac{\partial^2 \psi}{\partial v^2} + \frac{\gamma b}{g^2(\tau)} \left(\frac{\partial \psi}{\partial u} - \frac{\partial \psi}{\partial v} \right) = \sin \psi \qquad (3)$$

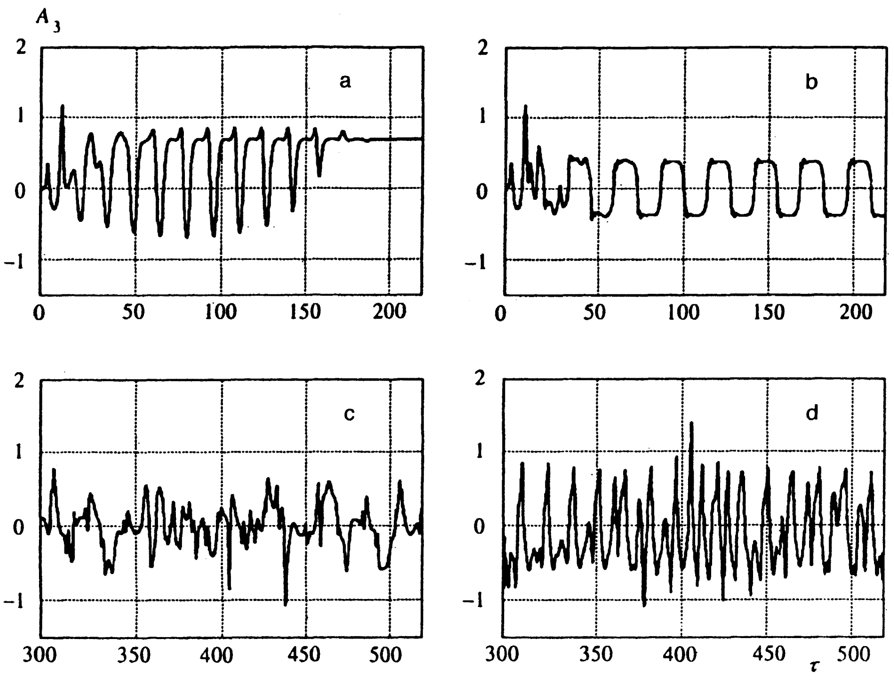

FIG. 1. Dependence of the amplitude $A_3(l,\tau)$ at the output on the time for $\gamma=0.3$, $R^2=0.022$ (a), $\gamma=0.3$, $R^2=0.95$ (b), $\gamma=0.2$, $R^2=0.95$ (c), $\gamma=0.105$, $R^2=0.95$ (d), and $l=10$.

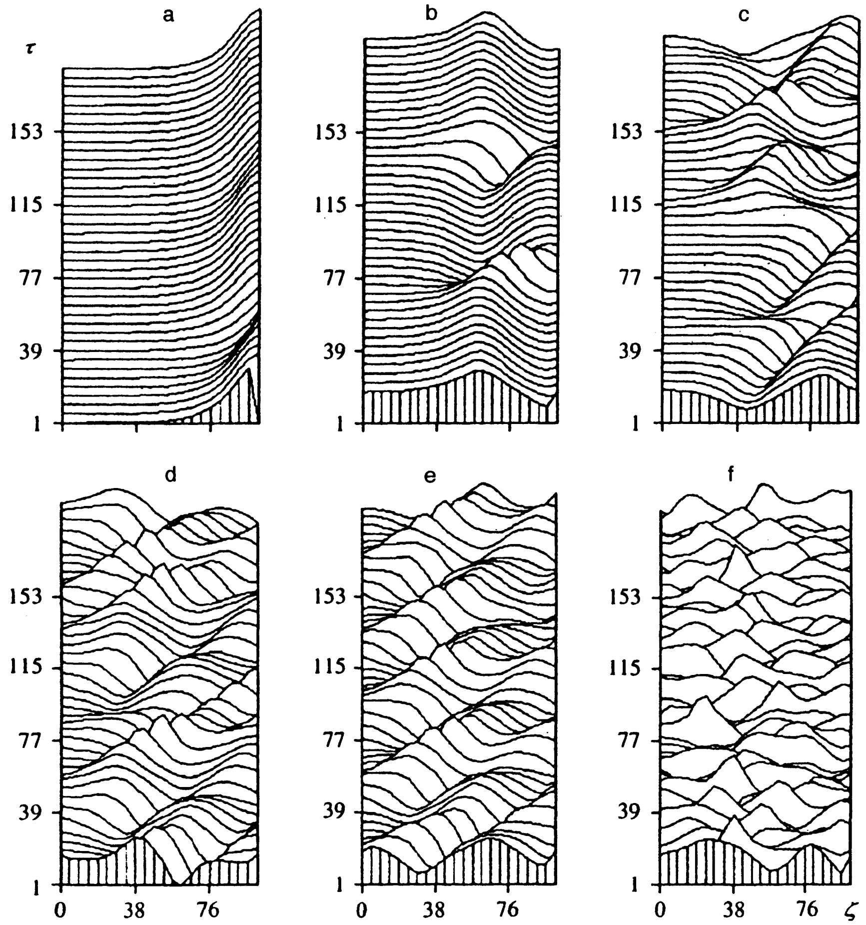

FIG. 2. Different regimes of the space–time dynamics of $A_3(\zeta,\tau)$ for $\gamma=0.3$, $R^2=0.022$ (a), $\gamma=0.3$, $R^2=0.95$ (b), $\gamma=0.2$, $R^2=0.95$ (c), $\gamma=0.105$, $R^2=0.95$ (d), $\gamma=0.077$, $R^2=0.95$ (e), $\gamma=0.05$, $R^2=0.95$ (f); $l=10$.

and thus interpret the stable excitations in the medium as solitons.

However, in a bounded medium such a transition does not lead to a simplification, since the boundary conditions in such a case must be satisfied at traveling boundaries. Moreover, the presence of absorption and nonideality of the reflection means that we cannot exploit the properties associated with the complete integrability of this equation.[5,8] Nevertheless, in the case of weak absorption, $\gamma \ll 1$, we note the single-soliton solution of (2)–(3) of the form $A_3 = b$ sech u, which reflects the specific nature of soliton formation. In the unmodulated case ($g^2=1$), we obtain for the soliton velocity the expression $1-1/b^2$, from which it follows that at small amplitudes ($|b|<1$) the peak of the soliton moves to the left (this is due to the displacement of the depletion front of the pump wave), while at larger amplitudes ($b>1$) the soliton moves to the right. For $|b|\cong 1$, the soliton will be decelerated until its amplitude is changed as a result of the evolution. Therefore, if a linear pulse is trapped into the soliton regime, the corresponding segment of its trajectory in the $\zeta\tau$ plane will have a characteristic S shape. We found such trajectories in all dynamical regimes, but it was only in the regular cases that these segments formed structures.

3. HIGH-FREQUENCY PUMPING

We consider first the case when the powerful wave has the higher frequency, the relations $f_1(\tau)=1$ and $f_2(\tau)=0$ holding (the wave at the frequency ω_2 is generated in the course of the interaction). In this case, the system (2) acquires the form

$$\left(\frac{\partial}{\partial\zeta}+\frac{\partial}{\partial\tau}+\gamma\right)A_3=0.5\,\sin(2\varphi),\qquad \varphi=\int_0^{\zeta}A_3(\zeta,\tau)d\zeta. \tag{4}$$

From (4), we determine the conditions of instability, making the assumption that $|A_3|$ and $|\varphi|$ are much less than unity and proportional to $\exp[i(\omega\tau-k\zeta)]$. After simple calculations, we can write the threshold condition in the form $\gamma<\gamma_{th}=-0.75\beta+0.25\,\mathrm{Im}\,\sqrt{\Delta}$, where $\beta=-\ln R^2/l>0$, $\Delta=(2n\pi/l+i\beta)^2-8$, $n=0,1,2,\ldots$ For small $\beta\ll 1$, we must have $\sqrt{2}l/\pi>n$. The minimum threshold is possessed by the mode with $n=0$ (aperiodic instability), and when $\beta\ll 1$ we have $\gamma_{th}\approx 0.707$ for it. For the general case when $n=0$, we write the threshold condition in the dimensional form

$$E_0^2>E_{th}^2=\frac{1}{\alpha K k_2 L^2}\left(2\Gamma L+\ln\frac{1}{R^2}\right)\left(\Gamma L+\ln\frac{1}{R^2}\right). \tag{5}$$

It follows from (5) in particular that the threshold will increase with decreasing reflection or decreasing length of the region. Note that for $R_0R_l<0$ (antisymmetric reflection, i.e., phase shift through π upon reflection by one of the boundaries) it is necessary to make the substitution $n\rightarrow n$

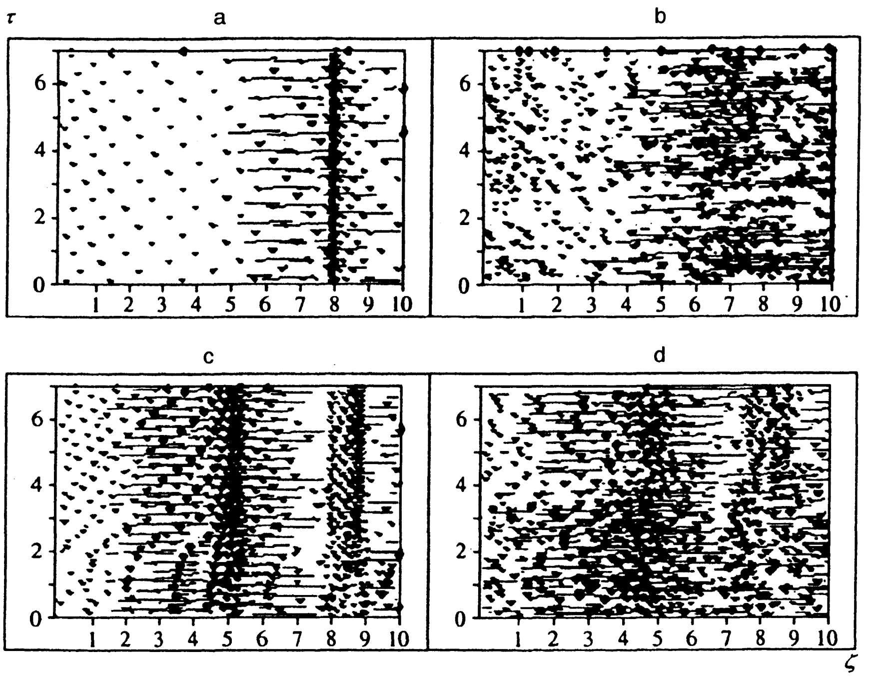

FIG. 3. Space–time trajectories of defects [the zeros of $A_3(\zeta,\tau)$] in the dynamical regime for different supercriticalities: a) $\gamma=0.3$; b) $\gamma=0.2$; c) $\gamma=0.105$; d) $\gamma=0.077$; $l=10$.

$+0.5$ in the expressions given above. Then for $n=0$ we have the condition $l > \pi/\sqrt{8}$, which determines the minimum length l of the region.

For $\gamma<\gamma_{th}$, the perturbations grow exponentially, and the system enters the nonlinear regime. Since in the general case it is very difficult to obtain an analytic solution of the nonlinear system (4), we made a computer experiment, solving this system numerically for various parameters. This made it possible to investigate in a unified framework all stages of the interaction from the initial instability to the developed nonlinear regime. For the calculations, we used $f_3(\tau)=f_{30}\exp[-(\tau-2)^2]$, $f_{30}=0.05$, $A_{30}=0$ for various l, R^2, and values of the supercriticality parameter γ from 0.7 to 0.001. The calculation was made using a high-order scheme, and the accuracy was tested by reducing the mesh step. The results are presented graphically.

We consider first the unmodulated case $f_1=1$.

As the calculation showed, the system exhibits very varied behavior depending on the values of γ, the length l, and the reflection coefficients R^2 (the strength of the feedback). Since the small boundary or initial disturbance was taken to be quite localized, under subcritical conditions with $\gamma>\gamma_{th}$ the system relaxes after a certain transient time to the trivial solution $A_1=1$, $A_{2,3}=0$.

However, as the supercriticality is changed ($\gamma<\gamma_{th}$), this solution is found to be unstable, and the system goes

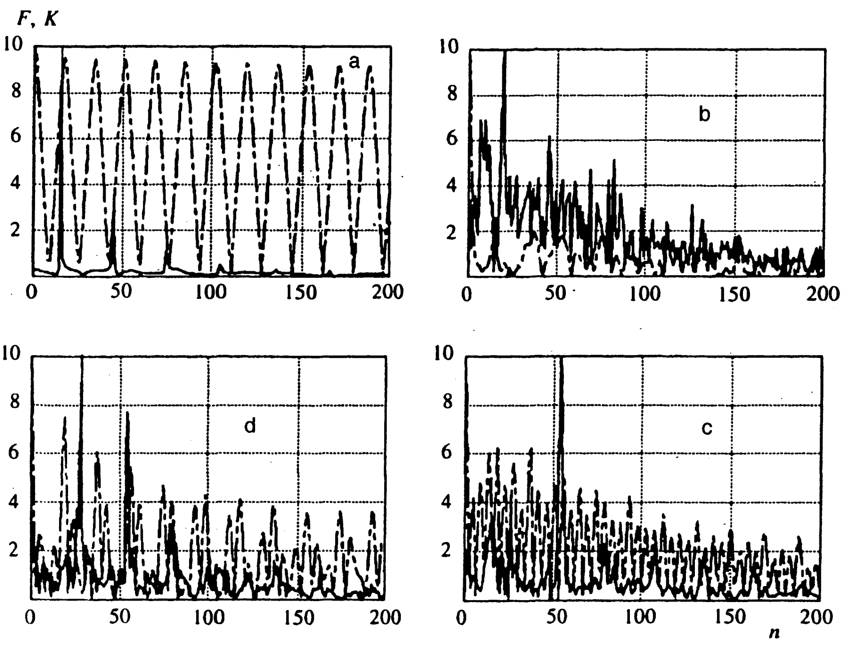

FIG. 4. The Fourier spectrum (F is the Fourier amplitude) and the autocorrelation function (K, dashed curve) of $A_3(l,\tau)$ as a function of the number of the time sample for $\gamma=0.3$ (a), $\gamma=0.2$ (b), and $\gamma=0.105$ (c) for an unmodulated pump and $\gamma=0.2$ for a modulated pump (d); $R^2=0.95$, $l=10$.

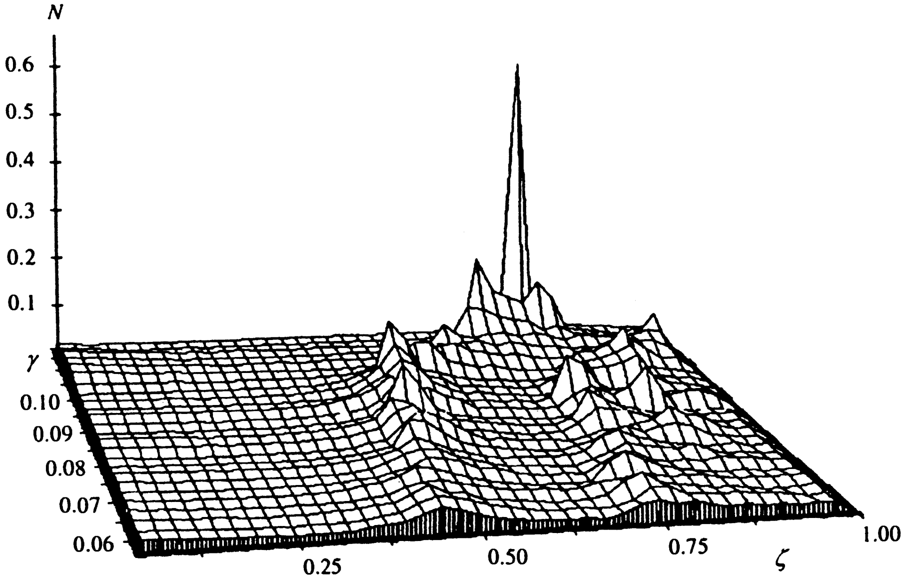

FIG. 5. Time-averaged distribution N of defects over the length as a function of the supercriticality γ for $R^2=0.95$, $l=10$.

over into a nonlinear stationary or dynamical regime of generation of oscillations. At the same time, $\varphi(l)\sim\pi/2$, and, therefore, it is no longer possible to ignore the nonlinearity of the interaction. Typical pictures of the space–time dynamics are presented in Figs. 1 and 2.

Figures 1a and 2a show the evolution of A_3 for $\gamma=0.3$ when $l=10$ and $R^2=0.22$ (after the transient). In this case, stationary amplitudes are established in the system in an oscillatory manner. During the transient, the solitons that have been formed leave the region but then are decelerated more and more until they come to a stop near the boundary. Such stationary states can also be found from (4) by setting $\partial A_3/\partial\tau=0$, as a result of which we obtain the equation of a mathematical pendulum with the subsidiary constraint

$$R^2=|A_3(0)e^{\gamma l}/A_3(l)|<1.$$

However, the corresponding solutions are stable only for small R^2. With increasing R^2, there develops in the system a dynamical regime in which it is not possible to ignore the derivative $\partial A_3/\partial\tau$. Such a situation has a general nature.

Figures 1b and 2b show the space–time dynamics for $\gamma=0.3$. In the initial stage, we see here the generation of a soliton. As the amplitude increases, the pulse is decelerated, acquires a stationary form, and then rapidly leaves the region. However, after the multiply-reflected part has arrived, the conditions that lead to the formation of a soliton are again fulfilled. Nonsoliton additions that detach themselves from the pulse are the first that return to the region. Since this part of the excitation is very nonstationary, the regime in which the contribution of these corrections is large acquires irregular features.

In the case of weak reflection, the arriving pulses have a phase-matching effect on the formation of the solitons. However, with increasing supercriticality and amplitude of the multiply reflected nonsoliton additions, the process of formation becomes more and more complicated. The fluctuations at the output acquire a complicated time dependence.

During the space–time evolution, and also as a result of the multiple reflection, which plays the role of a delayed feedback, the form of the excitations changes appreciably. It is very difficult to distinguish between amplitude and phase distortions of the waves. However, having in mind a comparison of our data with experiment,[3] we shall characterize the phase defects by the neighborhood of the zeros of the amplitude $A_3(\zeta,\tau)=0$ (at the given points, the phase

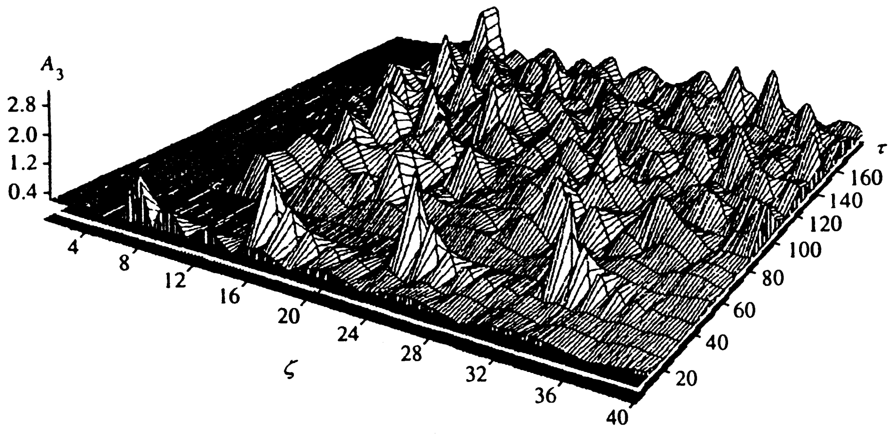

FIG. 6. Space–time dynamics of $A_3(\zeta,\tau)$ in the case of a large length of the region for $\gamma=0.1$, $R^2=0.001$, $l=40$.

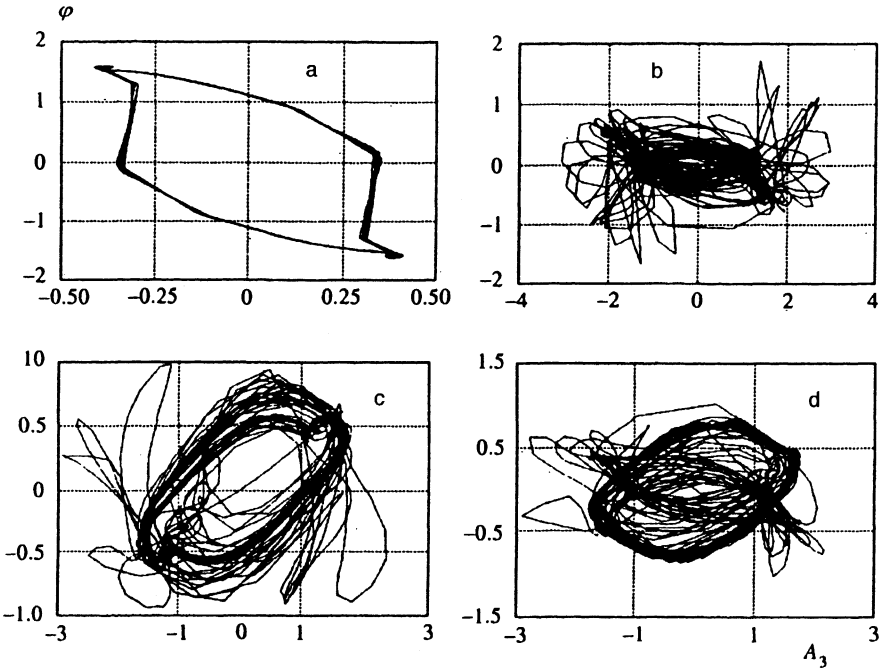

FIG. 7. Phase trajectories in the $|\varphi(l,\tau),A_3(l,\tau)|$ plane for $\gamma=0.3$ (a), $\gamma=0.2$ (b), and $\gamma=0.105$ (c) for unmodulated pumping and $\gamma=0.2$ for modulated pumping (d), $l=10$.

changes abruptly by π). As is shown in Ref. 3, these phase defects are manifested precisely in the region of small amplitudes. In recent theoretical work, such points have been associated with space–time defects of the wave field, reflecting the specific features of dynamical processes in nonlinear media.[1,2]

Depending on the supercriticality, our calculations revealed the existence of richer arrangements of such defects, both structured (as in Ref. 3) and irregular. The disposition of the maxima and minima of $A_3(\zeta\tau)$ had a similar structure.

The calculation shows that in the case of low supercriticality, when at the output of the system periodic nearly rectangular oscillations are established, the number of defects is small. With decreasing γ, the number of defects increases, and at $\gamma=0.3$ they are formed into a clearly distinguishable stationary structure (Fig. 3a).

However, a further decrease of γ to 0.2 leads to an abrupt rearrangement of the picture: the given structure is destroyed (Fig. 2b), and the oscillations at the output become irregular (Fig. 1c). With a further decrease ($\gamma=0.105$), a new more complicated structure takes shape in the system (Fig. 3c). The oscillations at the output become quasiperiodic but are interrupted by random surges (Fig. 1d).

Further advance into the above-threshold region leads to the formation of an ever more complicated network of structures, the rearrangement of which is accompanied by chaotic oscillations. At the same time, the number of defects increases, while the distance between them and, hence, the space–time scale of the structures, decreases. The system becomes very sensitive to a change in γ. Note that with allowance for the direction of the axes Figs. 3a and 3c are similar to the corresponding graphs of Ref. 3.

Since complicated oscillations accompanying the rearrangement of the structures could also arise from a series of oscillations with incommensurate frequencies, we also analyzed the spectrum. Figure 4 shows the Fourier spectra and autocorrelation functions for $A_3(l,\tau)$ for different γ. It can be seen that in the ordered phase the oscillations are narrowband (Figs. 4a and 4c), and it is only for $\gamma=0.2$ (Fig. 4b) that the spectrum has a typical noise form and the characteristic correlation time is very short, clearly indicating chaotic

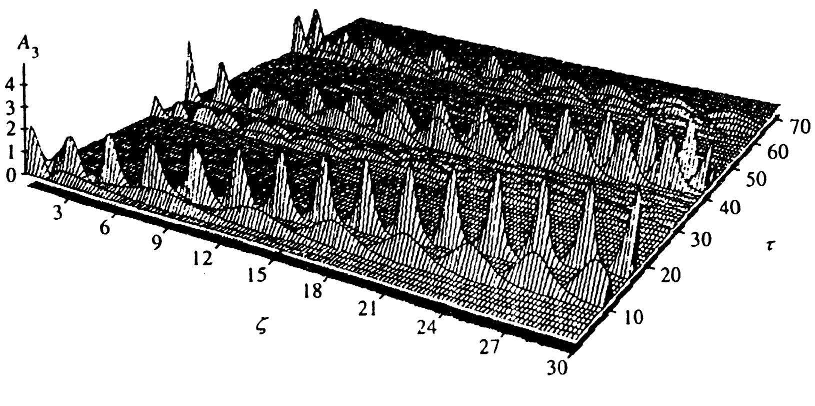

FIG. 8. Space–time dynamics of $A_3(\zeta,\tau)$ for the case of pumping at an intermediate frequency for $\gamma=0.002$, $R^2=0.95$, $l=30$.

dynamics in the system. Raising the sample rate confirms this conclusion.

The graphical results presented in Fig. 5 make it possible to trace the time-averaged distribution of the defects over the length as a function of the supercriticality for fixed strength of the reflection. For $\gamma \cong 0.3$, the defects accumulate at a single point $\sim 0.8l$. However, with increasing supercriticality the corresponding peak is destroyed, breaking up into two peaks of lower height. This corresponds to the formation of a new structure. This rearrangement occurs abruptly at $\gamma \cong 0.2$ and to a certain degree is similar to a phase transition; therefore, the noise is probably large here.

What we have said above applied mainly to the intermediate case, in which the length of the region was of the order of several half-widths of the solitons. Figure 6 presents a case of large length $l=40$, which demonstrates both the soliton dynamics of the transient process and the generation of a region of turbulence. It can be seen from Fig. 6 that after the first soliton has moved away processes of creation of new pulses stimulated by the multiple reflection of the nonsoliton oscillations commence. As a result, the generation becomes chaotic, and the generation region becomes a turbulence zone.

To elucidate the role of pump modulation, we consider the simplest case $f_1(\tau)=1-0.2\sin[0.01(\tau-2)]$ for $\gamma=0.2$ and times in the range 0–1200. In Figs. 4b and 4d and 7b and 7d, it can be seen that as a result of the modulation the spectrum and phase trajectory are significantly altered. Depending on whether $f_1(\tau)<1$ or $f_1(\tau)>1$, the trajectory either devolves into a limit cycle or acquires a very complicated form. The calculation showed that a change in the reflection coefficients R^2 leads to a similar picture.

The development of the chaotic regime in this medium probably occurs in accordance with the following scenario. Instability of the initial disturbances leads not only to the formation of a localized excitation but also to the creation of an extended chain of oscillations. There develops in the system a competition between two factors: parametric enhancement due to interaction with the pump wave and damping of the waves due to absorption. In a bounded medium, this latter circumstance also leads to damping of excitation energy upon reflection into the reverse wave. In the case of strong damping, the feedback that is established plays hardly any role, since the nonsoliton part already becomes very weak after two reflections. However, this part is important if the signal is appreciably amplified in the forward direction and is not too greatly attenuated in the reverse direction.

In the case of appreciable supercriticality, there is not sufficient time for the oscillator additions to be absorbed during the time of formation of the soliton, and the additions, *detached from the* pulse after reflection, arrive at the input of the system before the formation of the stationary excitation has been completed. As a result, the transient process begins with a new phase, and the resulting feedback leads to continuous mixing of the excitations. Because of the large difference of the phase velocities of the acoustic and electromagnetic waves, the local irregularities of the sound are carried over the interaction region, and a region of turbulence is generated in the system.

4. PUMPING AT INTERMEDIATE FREQUENCY

We now consider the case of pumping at an intermediate frequency ω_2, and we assume that $f_2(\tau)=1$, $f_1(\tau)=0$ (the wave at frequency ω_1 is generated during the course of the interaction). The system (2) takes the form

$$\left(\frac{\partial}{\partial\zeta}+\frac{\partial}{\partial\tau}+\gamma\right)A_3=0.5\sin(2\varphi),\quad \varphi=\int_0^\zeta A_3(\zeta,\tau)d\zeta+\frac{\pi}{2}. \tag{6}$$

As follows from (6), for small $A_3(\zeta,\tau)>0$ the right-hand side of the equation is negative. In this case, the medium is stable, and in the presence of damping or nonideal reflection all perturbations in the system will relax. The method of soliton relaxation is interesting (see Fig. 8). At short times, when the damping has not yet significantly changed its amplitude, the pulse maintains a stationary shape during its motion, emitting a nonsoliton part. However, as its amplitude decreases to a value $\cong 2$, the soliton begins to spread more and more rapidly, taking the shape of a breather. This is in agreement with Ref. 6, which noted the possibility of propagation of a small-amplitude breather in a partially bounded medium.

5. CONCLUSIONS

Thus, in the system considered above, with allowance for absorption and multiple reflection (delayed feedback), the picture of nonlinear interaction is very rich. In the case of a stable system (pumping at ω_2), the soliton exists after its formation for a finite time even in the presence of weak absorption and nonideality of the reflection. In the unstable case (pumping at ω_1), the development of instability can lead both to the formation of localized pulses and to superposition of a soliton and inhomogeneous oscillator complexes. Accordingly, in such a system both regular and chaotic oscillations can be observed. External modulation of the pump amplitude or a change in the reflection coefficients makes it possible to influence critically the wave dynamics, moving the system toward or away from some particular chaotic regime. Since the acoustic and electromagnetic subsystems are here coupled in a single system, from the experimental point of view such an effect can provide a unique opportunity to generate or eliminate chaotic behavior of not only acoustic oscillations but also of laser waves passing through a crystal.

[1]M. C. Cross and P. C. Hohenberg, Rev. Mod. Phys. **65** (2), 851 (1993).
[2]H. D. I. Abarbanel, R. Brown, J. J. Sidorovich, and L. S. Tsimring, Rev. Mod. Phys. **65**, 1331 (1993).
[3]G. Giacomelli, R. Meucci, A. Politi, and F. T. Arecchi, Phys. Rev. Lett. **73**, 1099 (1994).
[4]F. T. Arecchi, G. Giacomelli, A. Lapucci, and R. Meucci, Phys. Rev. A **45**, 4225 (1992).

[5]G. L. Lamb, Jr., *Elements of Soliton Theory*, Wiley, New York (1980).
[6]G. N. Burlak, V. V. Grimal'skiĭ, and N. Ya. Kotsarenko, Zh. Eksp. Teor. Fiz. **90**, 1487 (1986) [Sov. Phys. JETP **63**, 872 (1986)].
[7]A. S. Shcherbakov and I. B. Pozdnov, Pis'ma Zh. Tekh. Fiz. **20**, 12 (1994) [Tech. Phys. Lett. **20**, 5 (1994)].
[8]V. E. Zakharov, S. V. Manakov, S. P. Novikov, *et al.*, *The Theory of Solitons: The Inverse Scattering Method* [in Russian], Nauka, Moscow (1980).

Translated by Julian B. Barbour